

Supporting Information ID CC-COM-11-2013-048595

Two- and one-step cooperative spin transitions in Hofmann-like clathrates with enhanced loading capacity

L. Piñeiro-López, M. Seredyuk, M. C. Muñoz, J. A. Real

Synthesis. All chemicals were purchased from commercial suppliers and used without further purification.

Synthesis of bis(4-pyridyl)butadiyne (*bpb*). To a solution of CuCl (130 mg, 0.96 mmol) in pyridine (2–3 ml) under oxygen atmosphere was added 4-ethynylpyridine (600 mg, 5.81 mmol) with stirring and heated at 40–45°C for 2 h. The pyridine was removed at reduced pressure and the residual solid was washed with an aqueous solution of ammonium chloride (30 ml, 10%) and dissolved in chloroform. The organic layer was dried over MgSO₄, filtered and dried giving bis(4-pyridyl)butadiyne as lustrous dirty plates. The compound was purified by recrystallization from hot ethyl acetate to give yellowish lustrous plates (312 mg, 53 %). ¹H NMR (300 MHz, CDCl₃): δ 8.56 (4H, m, pyH^{2,6}), 7.64 (4H, m, pyH^{3,5}); ¹³C NMR (100 MHz, CDCl₃): δ 148.7, 128.6, 125.1, 79.2, 76.3. Elemental analysis calcd (%) for C₁₄H₈N₂: C, 82.33; H, 3.95; N, 13.72; found C, 82.53, H, 4.05, N, 13.69.

Synthesis of [Fe(*bpb*)Pt(CN)₄]·2naphthalene (1**) and [Fe(*bpb*)Pt(CN)₄]·2nitrobenzene (**2**).** Single crystals of **1** and **2** were grown using a slow diffusion technique. One side of a multi-arm shaped vessel contains (NH₄)₂Fe(SO₄)₂·6H₂O (20 mg, 51 mmol) dissolved in water (0.5 mL). The contiguous arm contains solid *bpb* (11 mg, 49 mmol) and guest (50 mg), and the third arm contains K₂Pt(CN)₄·3H₂O (22 mg, 51 mmol) in water (0.5 ml). The vessel was filled with a water/methanol (1:1) solution. Square shaped yellow (**1**) and brown (**2**) crystals suitable for single crystal X-ray analysis were obtained after 6 weeks.

Elemental analysis calcd (%) for **1** (C₃₈H₂₄FeN₆Pt): C, 55.96; H, 2.97; N, 10.30; found C, 55.59; H, 10.26; N, 3.10. EDAX calc. for **1**: Fe, 50.00; Pt, 50.00; found: Fe, 51.32; Pt, 48.68. Elemental analysis calcd (%) for **2** (C₃₀H₁₈FeN₈O₄Pt): C, 44.74; H, 2.25; N, 13.91; found C, 44.62; H, 1.92; N, 14.37. EDAX calc. for **2**: Fe, 50.00; Pt, 50.00; found: Fe, 48.76; Pt, 51.14.

The thermogravimetric analysis of **1** and **2** display two well defined loss of weight. The former at lower temperatures occurs in both compounds between ca. 415 K and 550 K and corresponds to the loss of two molecules of naphthalene or nitrobenzene. The second loss of weight taking place in the interval 625-840 K corresponds to the decomposition of the framework (see Figure 1 below).

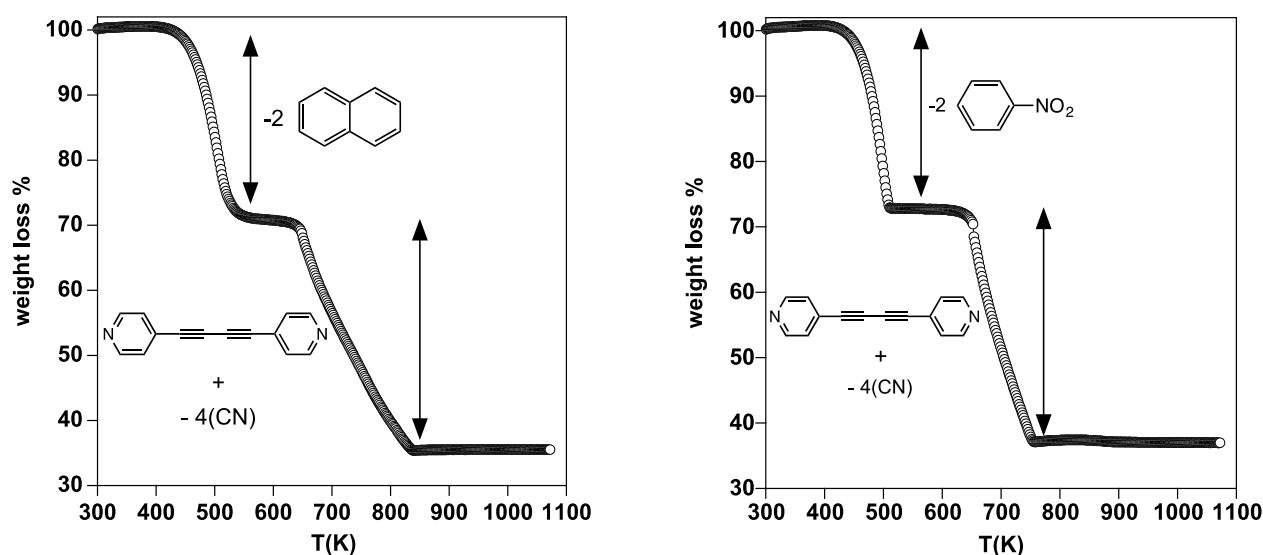


Figure S1. Thermogravimetric analysis of compounds **1** (left) and **2** (right).

Infra-red spectra of **1** and **2**.

The infrared spectra of **1** and **2** shown in Figures S2a and S2b, respectively clearly display the most characteristic features of both derivatives:

Compound 1: $\nu(\text{CNcyanide}) = 2161.2 \text{ cm}^{-1}$ (vs); $\nu(\text{C}=\text{Npyridine}) = 1602.0 \text{ cm}^{-1}$ (s); $\nu(\text{pyridine ring}) = 1418.7 \text{ cm}^{-1}$ (m); $\nu(\text{pyridine ring}) = 819.9 \text{ cm}^{-1}$ (s); $\nu(\text{naphthalene rings}) = 781.8 \text{ cm}^{-1}$ (vs); $\nu(\text{naphthalene rings}) = 541.6 \text{ cm}^{-1}$ (s); $\nu(\text{Pt-CN}) = 475.3 \text{ cm}^{-1}$ (s) (Figure S1a) (vs = very strong, s = strong, m = medium, w = weak).

Compound 2: $\nu(\text{CNcyanide}) = 2166.8 \text{ cm}^{-1}$ (vs); $\nu(\text{C}=\text{Npyridine}) = 1602.6 \text{ cm}^{-1}$ (s); $\nu(\text{pyridine ring}) = 1420.4 \text{ cm}^{-1}$ (m); $\nu_{\text{as}}(\text{NO}_2) = 1522.7 \text{ cm}^{-1}$ (vs); $\nu_s(\text{NO}_2) = 1346.1 \text{ cm}^{-1}$ (vs); $\nu(\text{pyridine ring}) = 852.8 \text{ (w), } 829.3 \text{ (s), } 793 \text{ (s) cm}^{-1}$; $\nu(\text{C}_6\text{H}_5\text{NO}_2) = 704.6 \text{ cm}^{-1}$ (s); $\nu(\text{Pt-CN}) = 466.7 \text{ cm}^{-1}$ (m) (Figure S1b) (vs = very strong, s = strong, m = medium, w = weak).

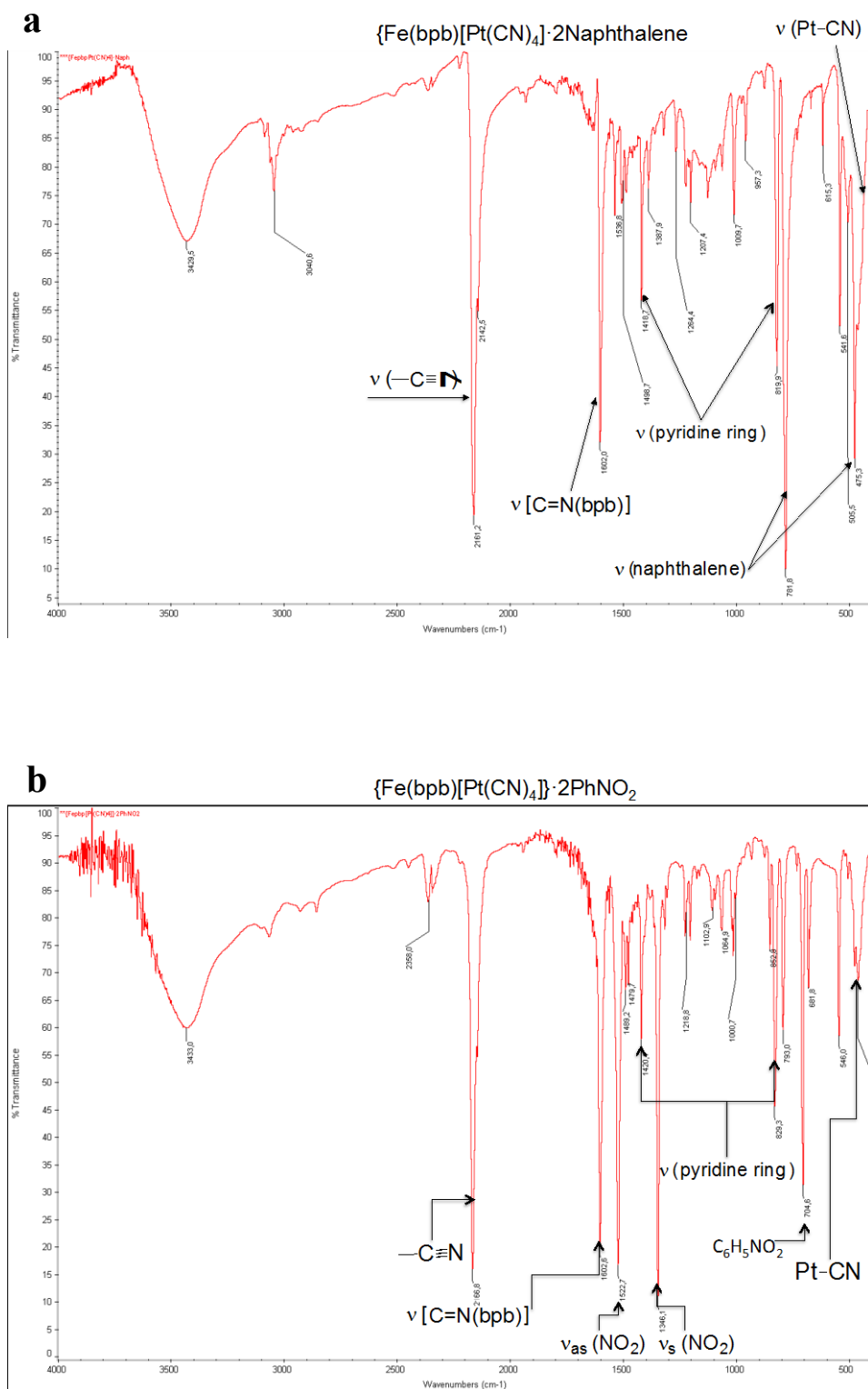


Figure S2. Infrared spectra of compounds **1** (a) and **2** (b).

Physical measurements

Variable-temperature magnetic susceptibility data were recorded on samples of **1** and **2** constituted of single crystals (10–15 mg) with a Quantum Design MPMS2 SQUID susceptometer equipped with a 7 T magnet, operating at 1 T and at temperatures 10–400 K. Experimental susceptibilities were corrected for diamagnetism of the constituent atoms by the use of Pascal's constants. TGA measurements were performed on a Mettler Toledo TGA/SDTA 851e, in the 150–400 K temperature range under a nitrogen atmosphere with a rate of 10 K min⁻¹. The thermodynamic parameters were analyzed with Netzsch Proteus software (Netzsch-Geraetebau GMBH). Analysis for C, H, and N were performed after combustion at 850 °C using IR detection and gravimetry by means of a Perkin–Elmer 2400 series II device. ¹H and ¹³C NMR spectroscopic measurements were done on an Advance DRX Bruker 300 MHz Spectrometer. IR spectra were recorded at 293 K by using a Nicolet 5700 FTIR spectrometer with the samples prepared as KBr discs.

Single crystal X-ray diffraction. Single-crystal X-ray data of **1** and **2** were collected on a Nonius Kappa-CCD single crystal diffractometer using graphite mono-chromated MoK_α radiation ($\lambda = 0.71073 \text{ \AA}$). A multi-scan absorption correction was performed. The structures were solved by direct methods using SHELXS-97 and refined by full-matrix least squares on F^2 using SHELXL-97.^[1] Non-hydrogen atoms were refined anisotropically and hydrogen atoms were placed in calculated positions refined using idealized geometries (riding model) and assigned fixed isotropic displacement parameters for **1** (120–250 K) and **2** (120 K). For compound **2** at 250 K only Fe and Pt atoms could be anisotropically refined. In general the crystals deteriorate as a consequence of the phase transition associated with the spin crossover transition. This is particularly more marked for compound **2** because the quality of the single crystals was systematically low. CCDC files 971021–971025 contain the supplementary crystallographic data for **1** (120 K), **1** (195 K), **1** (250 K), **2** (120 K) and **2** (250 K), respectively. These data can be obtained free of charge from The Cambridge Crystallographic Data Centre via www.ccdc.cam.ac.uk/data_request/cif.

¹ G. M. Sheldrick, SHELX97, Acta Cryst. A64, 112–122, 2008.

Table S1. Crystal data of compounds **1** and **2**.

	1		2	
Temperature (K)	120(1)	195(1)	250(1)	120(1)
Empirical formula	C ₃₈ H ₂₄ N ₆ PtFe			C ₃₀ H ₁₈ N ₈ O ₄ PtFe
Mr	815.57			805.46
Crystal system	triclinic			triclinic
Space group	<i>P</i> -1			<i>P</i> -1
<i>a</i> (Å)	7.2452(2)	7.3635(2)	7.5174(2)	7.2443(4)
<i>b</i> (Å)	13.9706(5)	14.1112(4)	14.3676(7)	13.8127(8)
<i>c</i> (Å)	16.3779(7)	16.3906(5)	16.350(2)	15.4746(9)
α (°)	73.531(3)	74.663(3)	76.831(8)	80.352(5)
β (°)	83.678(3)	82.349(2)	84.282(6)	87.669(5)
γ (°)	89.998(3)	89.878(2)	89.965(3)	89.842(5)
<i>V</i> (Å ³)	1579.24(10)	1626.86(8)	1710.5(3)	1525.26(15)
<i>Z</i>	2			2
<i>D</i> _c (mg cm ⁻³)	1.715	1.665	1.584	1.674
<i>F</i> (000)	796			780
μ (Mo-K _α)(mm ⁻¹)	4.921	4.777	4.544	5.105
Crystal size (mm)	0.08 x 0.12 x 0.12			0.06 x 0.08 x 0.08
No. of total reflections	10484	10926	7909	8234
No. of reflections [<i>I</i> >2σ(<i>I</i>)]	9658	9980	6281	7033
<i>R</i> ₁ [<i>I</i> >2σ(<i>I</i>)]	0.0505	0.0239	0.0921	0.0511
<i>R</i> ₁ [all data]	0.0553	0.0289	0.1160	0.0635
S	1.002	0.902	1.061	1.072
				1.161

$$R_1 = \sum \|F_O - |F_C|\| / \sum |F_O|; wR = [\sum [w(F_O^2 - F_C^2)^2] / \sum [w(F_O^2)^2]]^{1/2}.$$

$$w = 1 / [\sigma^2(F_O^2) + (m P)^2 + n P] \text{ where } P = (F_O^2 + 2F_C^2) / 3;$$

m = 0.0656 (**1 (120 K)**), 0.0273 (**1 (195 K)**), 0.1516 (**1 (250 K)**), 0.0580 (**2 (120 K)**) and 0.0621 (**2 (250 K)**);

n = 23.2445 (**1 (120 K)**), 1.3390 (**1 (195 K)**), 49.4900 (**1 (250 K)**), 4.6644 (**2 (120 K)**) and 0.0000 (**2 (250 K)**).

Table S2. Selected bond lengths [\AA] and angles [$^\circ$] for **1**.

	120 K	195 K	250 K
Fe(1)-N(1)	2.001(5)	2.000(2)	2.19(2)
Fe(1)-N(2)	1.934(4)	1.935(2)	2.10(2)
Fe(1)-N(6)	1.944(4)	1.938(2)	2.11(2)
Fe(2)-N(3)	1.935(4)	2.124(2)	2.13(2)
Fe(2)-N(4)	1.938(4)	2.127(2)	2.11(2)
Fe(2)-N(5)	1.996(5)	2.229(2)	2.19(2)
N(1)-Fe(1)-N(2)	88.2(2)	88.62(8)	87.8(7)
N(1)-Fe(1)-N(6)	88.2(2)	88.33(8)	87.8(6)
N(2)-Fe(1)-N(6)	90.9(2)	92.13(8)	91.4(6)
N(3)-Fe(2)-N(4)	90.5(2)	90.05(8)	91.2(6)
N(3)-Fe(2)-N(5)	90.7(2)	89.60(8)	87.7(8)
N(4)-Fe(2)-N(5)	88.8(2)	88.99(8)	86.7(8)

Table S3. Selected bond lengths [\AA] and angles [$^\circ$] for **2**.

	120 K	250 K
Fe(1)-N(1)	2.000(5)	2.199(12)
Fe(1)-N(2)	1.933(5)	2.167(12)
Fe(1)-N(6)	1.934(5)	2.141(12)
Fe(2)-N(3)	1.934(5)	2.161(12)
Fe(2)-N(4)	1.937(5)	2.144(13)
Fe(2)-N(5)	1.997(6)	2.232(15)
N(1)-Fe(1)-N(2)	88.4(2)	89.0(4)
N(1)-Fe(1)-N(6)	88.2(2)	88.4(4)
N(2)-Fe(1)-N(6)	91.1(2)	90.7(5)
N(3)-Fe(2)-N(4)	89.7(2)	89.2(5)
N(3)-Fe(2)-N(5)	89.2(2)	89.3(5)
N(4)-Fe(2)-N(5)	89.8(2)	89.8(5)

Table S4. Short contacts between invited molecules and *bpb* in **1**.

C atoms	Distance C···C/Å		
	120 K (LS–LS)	195 K (LS–HS)	250 K (HS–HS)
<i>bpb</i> ···naph 1 (blue)	C(19)···C(13)	-	3.624(7)
	C(23)···C(13)	-	3.656(4)
	C(24)···C(13)	3.553(10)	-
	C(24)···C(14)	3.499(11)	-
	C(25)···C(12)	3.546(11)	-
	C(25)···C(13)	3.560(12)	-
	C(25)···C(14)	3.646(13)	-
	C(26)···C(1) (T-Shaped)	3.670(11)	-
	C(26)···C(14)	-	3.628(6)
	C(2)···C(30)	-	3.609(5)
<i>bpb</i> ···naph 2 (red)	C(2)···C(31)	-	3.510(10)
	C(1)···C(32)	-	3.620(10)
	C(2)···C(32)	-	3.519(5)
	C(1)···C(33)	-	3.572(4)
	C(3)···C(34)	3.589(11)	-
	C(4)···C(35)	3.491(12)	-
	C(4)···C(36)	3.482(13)	-

Table S5. Short contacts between invited molecules and *bpb* in **2**.

C atoms	Distance C···C/Å	
	120 K (LS)	250 K (HS)
<i>bpb</i> ···phNO ₂ 1 (blue)	C(1)···C(23)	3.657(12)
	C(13)···C(19)	3.646(12)
<i>bpb</i> ···PhNO ₂ 2 (red)	C(1)···C(23)	3.657(12)
	C(13)···C(19)	3.646(12)
	C(13)···C(27)	3.685(11)
	C(13)···C(28)	-
	C(14)···C(28)	3.693(11)
	C(11)···C(29)	3.527(12)
		3.518(38)

Table S6. Mössbauer parameters, isomer shift (δ , relative to -iron), quadrupole splitting (ΔE_Q), half-width of the lines ($\Gamma_{1/2}$) and percentage of the multiplet populations in the HS and LS states (A) at different temperatures for **1** and **2**.

Compound	T/K	Doublet	$\delta/\text{mm s}^{-1}$	$\Delta E_Q/\text{mm s}^{-1}$	$\Gamma_{1/2}/\text{mm s}^{-1}$	$A/\%$
1	80	LS1	0.47(2)	0.32(1)	0.14(6)	50.0(1)
		LS2	0.49(2)	0.16(2)	0.16(7)	50.0(1)
	199	LS	0.47(1)	0.14(3)	0.13(2)	49.5(3)
		HS	1.11(2)	1.53(4)	0.16(2)	50.5(5)
	300	HS1	1.05(1)	0.51(2)	0.13(1)	45.9(3)
		HS2	1.06(1)	1.21(2)	0.15(1)	54.1(4)
2	80	LS1	0.47(1)	0.15(2)	0.12(2)	47.0(2)
		LS2	0.46(1)	0.33(3)	0.15(1)	53.0(2)
	300	HS1	1.07(1)	0.90(1)	0.14(1)	54.1(4)
		HS2	1.05(1)	0.30(1)	0.12(1)	45.9(3)

Figure S3. Projection of the crystal structure of **2** along *a* axis. Two types of invited nitrobenzene molecules are colored in red and blue.

